Effect of a Liner Material on the Formation of the Wrapping Explosively-Formed Penetrator

Q. Z. Xu, J. P. Yin,[1] Z. J. Wang, J. Y. Yi, and F. D. Dong

School of Mechatronic Engineering, North University of China, Taiyuan, China

[1] yjp123@nuc.edu.cn

The wrapping explosively-formed penetrator is a new approach to shape change based on a pre-folded double liner: outer liner of higher density forming the shell and the inner liner of lower density forming the core. The penetrator can not only penetrate the armor but can form lots of fragments behind the target when it attacks light armored objects. The fragments generated by the lateral enhanced effect are able to destroy crew and equipment improving the integrated damage outcome. The shape and materials of the core and shell are the main factors controlling the penetrability and formation of fragments. The effect of liner materials on penetration was studied. with AUTODYN analysis. The results show that the difference in the through-thickness velocities and the interface of the two liners are the main factors leading to the separation of the core and shell. Penetrator with an evident lateral enhanced effect could be helpful to choose appropriate liner materials. The feasibility of forming the penetrator with double liners is substantiated providing a reference for the selection of liner material.

Keywords: wrapping explosively-formed penetrator, double liners, lateral enhanced effect, combination of material, numerical simulation.

Introduction. The shaped charge warhead is the most effective weapon to attack armor targets. Its continuous development due to the escalation of armor targets is aimed at more efficient damage to it. The development of armor protection technology applied more and more armor protection to weapons and equipments. Armored vehicles, military helicopters and other light armor equipment, with its flexible mobility, have played an increasingly important role in modern war [1]. To incur loss in combat capability by destroying such light armor targets, its internal occupants and electronic equipments is the focus of research. The traditionally explosively-formed projectile has the characteristics of big perforation and long distance flight but their after effect is largely dependent on the characteristics of the target. The characteristics of shaped jet and jetting projectile charge (JPC) is the depth of penetration not the perforation or the after effect. Therefore, it is not suitable for such light armor. A penetrator with enhanced lateral effect (PELE) is an effective weapon against such light armor. It can effectively reach the enemy crew and equipment protected by armor due to armor-piercing and fragmentation [2, 3]. The range of PELE applicability is limited by available guns, which are used to launch them. The research on wrapping explosively-formed penetrator (WEFP) aims to retain the effect of armor-piercing and fragmentation of PELE and to solve the problem of poor applicability.

Many researchers have done a similar study on the generation of WEFP. Men et al. [4] had put forward a concept of wrapping explosively-formed compound penetrator (WEFCP), and succeeded in getting a combined penetrator with a high velocity by using metal liner wrapping active materials. Wang et al. [5] had analyzed the factors, which influenced the formation of WEFCP by numerical simulation and identified a number range of relevant parameters. Arnold et al. [6] introduced the WEFP concept and predicted its potential applications at the 28th International Ballistic Conference.

However, during the process of WEFP formation, the effect of liner material has not been studied in detail. This paper analyzed the process of forming WEFP and study effect

of liner material on the formation of WEFP. Such WEFP formed with suitable material had been found to be able to generate lateral enhanced effect while attacking the target. This article provides a reference for the design of anti-armor warhead.

1. Formation Theory of WEFP. The structure of double liners was designed as hemisphere with variable thickness and the density of outer liner was higher than inner liner. This is required to generate a penetrator with lateral effect. After the detonation wave swept over the surface of the liner, the element was accelerated and began to deform. The self-forging process and the final shape of the EFP were determined by the velocity of the element. The self-forging process of the liner came to an end until the velocity gradient of each element becomes zero [7]. The element at liner edge gained higher acceleration due to less mass at liner with thinner edge. The velocity gradient in axial and radial direction resulted in front folding formation. The higher density of shell resulted in the same lateral effect for WEFP as PELE when penetrated the targets.

2. Simulation Model and Parameters.

2.1. Structural Parameters of Shaped Charge. The diameter of the charge was 100 mm and length/diameter ratio was 0.6. Diameter of outer liner was 90 mm with the outer curvature radius 72 mm, inner curvature 81 mm and the thickness at the center was 4 mm. Diameter of inner liner was 90 mm with the outer curvature radius 81 mm and inner curvature 117 mm and the thickness at the center was 5 mm. Half structure diagram was shown as Fig. 1.
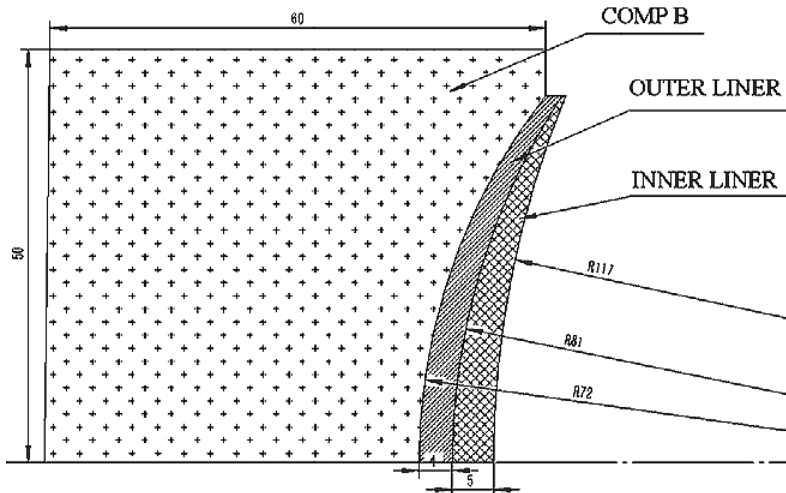
Fig. 1. Structure of charge.

2.2. Finite Model and Material Parameters. Euler algorithm was used for explosives and airspace selection in models. There is no distortion caused by large deformation of explosives. Lagrange algorithm was used for double liners because it can accurately describe the deformation behavior of the material and their relative movement. Euler domain was bound by the constraint of flow-out and coupled with liners through automatic fluid-solid coupling. Free contact algorithm was used to bind the two liners. The detonation point located at the center of end face of explosive.

The several materials selected in this paper were iron and its alloys, aluminum and its alloys and two kinds of nonmetallic materials. Iron and its alloys is the most common material and often used as liner. It can hold integrity in the process of formation, and it is easier to break after attacking target. This feature meets the requirements for the shell of WEFP. Four kinds of iron and its alloys, steel 1006, Armco iron, Iron CE, and steel 4340

were selected. These belong to four different types of iron alloys. There are suitable material modes in AUTODYN database to make simulation conveniently [8]. Aluminum is the most ordinary metal with density lower than iron. Nylon was selected because its density is similar with many nonmetallic materials. Another nonmetallic material was Teflon because of the much higher density than nylon.

The equation of state for air was ideal gas. The type of dynamite was COMP B with the Jones–Wilkins–Lee (JWL) equation of state for explosives. Parameters of explosive as shown in Table 1.

T a b l e 1

Parameters of COMP B

ρ, g/cm^3	D, km/s	P_{CJ}, GPa	A, GPa	B, GPa	R_1	R_2	ω	e_0, GPa	v_0
1.717	7.98	29.5	524.23	7.68	4.2	1.1	0.34	8.5	1.0

Equation of state for materials of liners is shock. Shock is the most commonly used equation for describing the mechanical properties of materials at high speed impact.

Several materials were selected for liners in next simulation. Three strength criteria, namely Johnson–Cook (JC), Steinberg–Guinan (SG), and von Mises, are used. The first two can describe the strength of material properties in the case of high temperature, high stress and high strain rate. These were often used in blast simulation. Two nonmetallic materials can be simply described by the von Mises criterion, as their yield strength can be ignored under blast conditions. Parameters of several materials are shown in Tables 2–4.

T a b l e 2

Parameters of JC Model

Material	Parameter								
	G, GPa	ρ, g/cm^3	A, GPa	B, GPa	n	C	m	T_m, K	T_r, K
Steel 1006	81.8	7.896	0.350	0.275	0.36	0.022	1.00	1811	300
Armco iron	80.0	7.890	0.175	0.380	0.32	0.060	0.55	1811	293
Iron CE	80.0	7.890	0.290	0.339	0.40	0.055	0.55	1811	300
AL2024-T351	27.6	2.785	0.265	0.426	0.34	0.015	1.00	775	300
Steel 4340	81.8	7.830	0.792	0.510	0.26	0.014	1.03	1793	300

T a b l e 3

SG Specific Parameters of Material

Material	ρ_0, g/cm^3	G_0, GPa	Y_0, GPa	Y_{max}, GPa	γ_0	a	b	T_m, K
AL2024-T4	2.785	28.6	0.26	0.76	2	0.017	0.185	1220
AL1100-O	2.707	27.1	0.04	0.48	1.97	0.002	1.767	1220

T a b l e 4

Specific Parameters of Two Nonmetallic Materials

Material	ρ, g/cm^3	γ_0	C_1, m/s	G_0, GPa	Y_0, GPa
Nylon	1.14	0.87	2290	3.68	0.05
Teflon	2.16	0.9	1340	2.33	0.05

3. Formation and Analysis of Single Liner with Different Material.

3.1. Forming Results and Analysis of Several Iron Alloy Liners. The same structure of charge and finite model, except for the absence of the inner liner, are used. Two grades of iron (Iron CE and Armco iron) and two grades of steel (1006 and 4340) were selected for the outer liner material, and their behavior under detonation was examined. 150 μs after detonation, the formation and speed of penetrator had been steady, and were shown as Table 5.

T a b l e 5

Formation and Speed of Ferruginous EFP

Material	Steel 1006	Iron CE	Armco iron	Steel 4340
Velocity (m/s)	1834	1835	1838	1854
Shape of EFP				

It can be seen from Table 5 that the velocities of penetrators with steel 1006 and iron CE were the lowest (1834 and 1835 m/s, respectively) and the degree of their compression in the radial direction implied a good compactness of the projectile. The projectile prepared from armco iron had a speed of 1838 m/s, with a somewhat larger opening front due to a lesser degree of compression in the radial direction. The last projectile prepared from steel 4340 had the highest speed of 1854 m/s, but its radial compactness was the worst. There was a large opening front and the smallest length/radius ratio. The shell of WEFP is usually produced from iron and its alloys due to their high density. Furthermore, the WEFP formation had to exhibit a good wrapping, so that the radial compactness of projectiles utilizing armco iron and steel 4340 fails to fit these wrapping requirements. Hence, steel 4340 and armco iron were excluded from the further analysis.

3.2. Aluminous Forming Results and Analysis. Three kind of aluminous materials were chosen, AL2024-T351, AL2024-T4, and AL1100-O. The density of aluminous materials is lower than iron but higher than the two nonmetallic materials, Teflon and nylon. Therefore, it could be inner material combined with iron or be outer liner material combined with the two nonmetallic materials. The single aluminum liner's formation at the time of 150 μs after detonation is shown in Table 6.

As shown in Table 6, the velocity of AL2024-T351 was similar with AL2024-T4, about 3202 m/s, and slightly lower than the speed of AL1100-O. During the process of formation, the edge of AL2024-T351 liner fails to collapse along a symmetric axis because of the slight radial velocity, so that the elements are extruded into a bulge. The radial compactness and axial extension of AL2024-T4 was the worst, resulting in a dish shape. The AL1100-O liner produced a compact projectile with a higher length/radius ratio

T a b l e 6

Formation and Speed of Aluminous EFP

Material	AL2024-T351	AL2024-T4	AL1100-O
Velocity (m/s)	3204	3202	3222
Shape of EFP			

because the elements of liner were compact in the radial direction, while the radial velocity was converted into the axial deformation and extension. According to the analysis and comparison among the three aluminous projectiles, AL1100-O and AL2024-T351 materials are more suitable as liner materials.

Iron is a strain rate-sensitive material. Therefore, its yield strength will increase due to strain hardening under detonation, insofar as the strain rate and temperature have a great effect on the dynamic performance of aluminum [9, 10]. The static parameters of the material cannot intuitively reflect the deformation of the material in the high temperature, high pressure and large strain rate environment. According to the simulation of single liner, the deformation behavior of different materials under detonation can be observed clearly and it provides an effective reference to the selection of material in double liners.

4. Simulation and Analysis of the Forming of WEFP.

4.1. Simulation and Analysis of the Forming of WEFP with One Material. Although the density of inner liner should be lower than outer liner in order to prepare a WEFP with lateral effect. It is necessary to simulate the progress of double liners with one material for studying other factors such as speed gradient in axial and radial, free interface between two liners. AL1100-O was selected as the material of double liners. Gauges points numbered *1* to *5* were set up along the bus bar in the middle of outer liner. Gauges points numbered *6* to *12* were set up in the direction of thickness on double liners (point number *6* to *8* were laid on outer liner and number *9* to *12* on inner liner). The formation process of double liners and positions of gauges points are shown in Fig. 2. The speed–time curves of gauges points are depicted in Fig. 3.
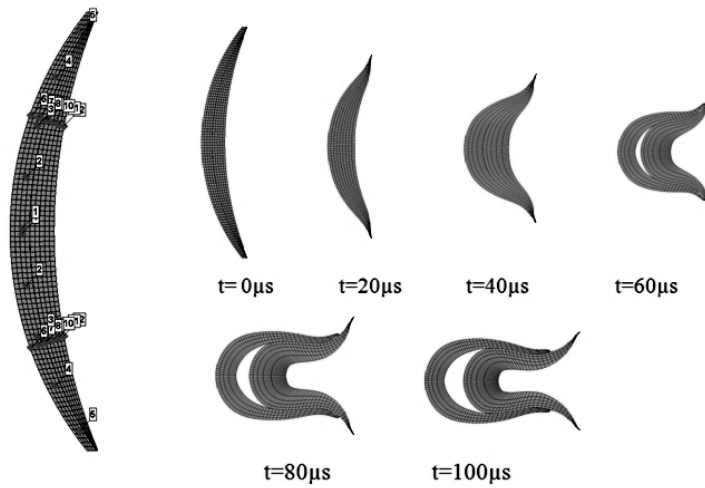
Fig. 2. Formation process of double liners and layout of gauges points.
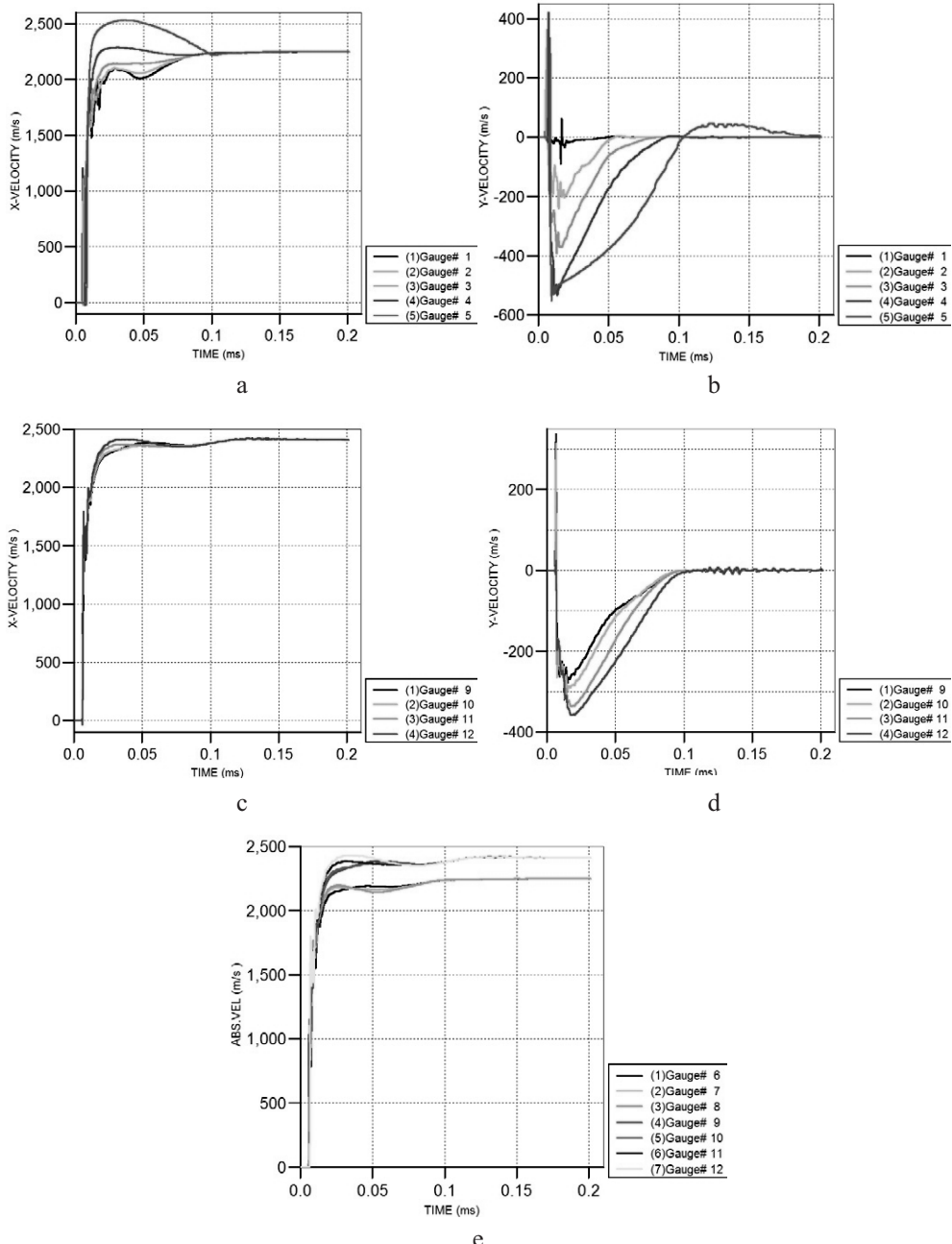
Fig. 3. Speed of gauges points: axial (a) and radial (b) speed of gauges points *1* to *5*; axial (c) and radial (d) speed of gauges points *9* to *12*; (e) speed of gauges points *6* to *12*.

From Fig. 2, one can observe the formation process of double AL1100-O liners. The edge of the liners has produced a significant radial compression and axial stretching but no gap is observed at 40 μs. A clear gap is observed between the top of liners at 60 μs, which grows larger with time. The deformation of double liners is found basically over 100 μs and most part of inner liner has disengaged from the outer liner. The two liners are then completely separated by the difference in the axial velocities.

From Fig. 3a, one can see the difference of axial velocity among elements along the bus bar. The initial axial velocity is smaller during detonation effect stage, and the elements become closer to the top of liner. The elements have been accelerated to the maximum velocity at 30 μs. Corresponding the gauges points, from *1* to *5*, the axial velocity was found to be 2094, 2096, 2140, 2288, and 2527 m/s, respectively. The difference in axial velocity among elements is basically disappeared at 100 μs and the axial tension of liner is finished. As we can see from Fig. 3b, the variation law of the radial velocity is similar to that of the axial velocity but the time is almost 15 μs early. According to analysis the difference among the elements in the direction of thickness is evident from Fig. 3c and 3d. The elements closer to the inner wall have greater radial and axial velocity. The axial velocity difference reached to the maximum value at 30 μs and it was found to be about 93 m/s between gauges point *9* and *12*. The difference in radial velocity was earlier found to be the maximum, about at 16 μs. And at this time, the different value between gauges point *9* and *12* are found to be 97 m/s. From Fig. 3e, the speed of two liners basically reaches a stable value at 30 μs. The average speed of inner and outer liner is found about 2394 and 2270 m/s, respectively. The difference of velocity between gauges point *8* and *9* are about 135 m/s obviously more than the difference value between them at the same part. Therefore, the difference of velocity in the direction of thickness and the free interface between two liners is the primary factors leading to separation of double liners.

4.2. Simulation and Analysis about Formation of WEFP with Various Material Combinations. According to the conclusion in Section 4, six schemes were designed to study the material combination effect. 150 μs after detonation, the formation and velocity of WEFP have reached steady state and been shown in Table 7 (separation means the inner liner's top beyond the tail of the outer liner in the axial direction).

By comparing Plan 1 with Plan 2, one can see that the shape of formation and velocity are almost identical. The speed of outer/inner liner was 1465 and 1693 m/s, respectively. The only difference is the material of outer liner which is steel 1006 and iron CE. It is evident that the behavior of steel 1006 and iron CE under detonation is coincidence. The outer liner eventually formed a "cylinder-like" shell with one end closed. Radial compression of inner liner is insufficient, forming a "trumpet-like" opening. The inner liner is partially out of the outer liner but the two liners were not completely separated at 150 μs.

In Plan 3, the speed of the outer 1and the inner liner are 1526 and 1758~1775 m/s, respectively. The outer liner eventually formed a "cylinder-like" shell with one end closed and the length/radial ratio become more comparatively, suitable for wrapping. The inner liner becomes compact with basically stable speed. The two liners are not separated, and most of the inner liner was embedded in the cavity formed by the outer liner.

In Plan 4, the speed of outer and the inner liner are found to be 1654 and 1915 m/s. The edge part of the outer liner resulted in a "trumpet-like" front opening due to lack of pressure in radial. Inner cover becomes compact well within the radial. But the radial and axial velocity is less than the part nearby it so that the formation looked like a "mushroom head." The two liners are not separated but most of the inner liner had gone beyond the outer liner.

In plan 5, the speed of liners is compared with the previous several programs have increased significantly. The speed of inner and outer liner are 2403 and 2511~2531 m/s. In the aspect of forming shape, the outer liner eventually formed a "cylinder-like" shell with one end closed but the length/radial ratio is small comparatively. The inner liner is compact but there is an obvious cavity between two liners. The two liners are not separated and the inner liner was mostly embedded in the outer liner.

In plan 6, the outer liner speed was 2727 m/s and the inner liner speed was 2867 m/s. The length/radial ratio of outer liner was relatively small because of its large diameter. The inner liner is pressed compact with a big head and a small tail. The two liners are not separated, but the inner liner is beyond the outer liner partly.

T a b l e   7

The Simulation Results of 6 Schemes

Number of plan	Combination of materials	Velocity of outer liner (m/s)	Velocity of inner liner (m/s)	Separation state	Shape of formation
1	Iron CE + AL1100-O	1465	1694	Not separated	
2	Steel 1006 + AL1100-O	1466	1692	Not separated	
3	Steel 1006 + Teflon	1526	1758~1775	Not separated	
4	Steel 1006 + Nylon	1654	1915	Not separated	
5	AL2024-T351 + Teflon	2403	2511~2531	Not separated	
6	AL2024-T351 + Nylon	2727	2867	Not separated	

From the first two scenarios, it can be seen that aluminum is used as the inner liner material resulted in sufficient radial compression of inner liner with poor compact.

It can be seen from Plans 3 and 5. Teflon is suitable to be inner liner material because the core generated by inner liner is compact in radial and stretched well in axial. And two materials combined with it are all forming a "cylinder-like" shell which is appropriate for wrapping.

According to Plans 4 and 6, it can be seen that nylon selected as inner liner material is seemed as a "mushroom head."

In generall, the strength of liner material has an effect on the formation and velocity distribution of WEFP.

5. Assessment of Formation. The advantages of WEFP are the abilities of expanding hole by lateral effect when penetrating targets and forming lots of fragments to enlarge the damage area. Therefore, lateral effect of WEFP is an important index to evaluate whether the formation is desirable. According to the formation of Section 5, schemes 2, 3, 4, 5, and 6 are arranged to penetrate a steel 4340 target whose thickness was 20 mm at 150 μs after detonation. The effect of reaming is evaluated by η,

$$\eta = (d_{ex} - d_{mi})/d_{mi},$$

where d_{ex} is the diameter of the exit and d_{mi} is the smallest size of diameter.

T a b l e 8

The Results of Reaming of Different Plans

Number of plan	Combination of material	d_{mi}, mm	d_{ex}, mm	η, %
2	Steel 1006 + AL1100-O	43.6	57	30.7
3	Steel 1006 + Teflon	38.6	49.8	29
4	Steel 1006 + Nylon	36.6	51.4	40.4
5	AL2024-T351 + Teflon	52.6	63.5	19.8
6	AL2024-T351 + Nylon	55.6	61.6	10.8

| t=15μs | t=17μs | t=19μs | t=21μs | t=23μs |
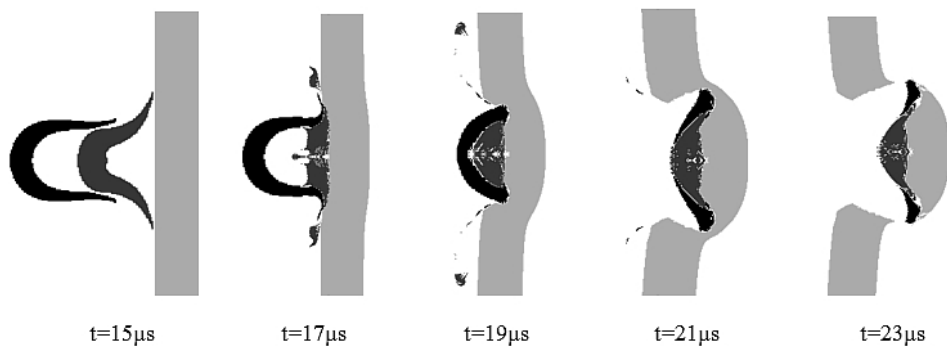
Fig. 4. The penetrating process of WEFP generated by plan 2.

The penetrating process of plan 2 was shown in Fig. 4. The results of reaming of different plans were shown in Table 8.

From Fig. 4, it can be seen that WEFP with a good formation shows a strongly manifested lateral effect when penetrating the target. The penetrator expanded in the radial direction and the exit hole got enlarged. According to the data listed in Table 8, the lateral penetration effect of WEFP with steel 1006 used as the outer liner material is stronger than that with aluminum. The plan 4 is the best in reaming with $\eta = 40.4\%$. The reaming effect of WEFP with an aluminum shell was more feeble, with the highest value of 19.8%.

C o n c l u s i o n s

1. According to the simulation of a single liner, the deformation behavior of different materials under detonation was studied and provided an effective reference for the selection of material in double liners.

2. The difference of velocity in the direction of thickness and the free interface between two liners are the primary factors leading to the separation of double liners.

3. The strength of a liner material is critical for the formation and velocity distribution of WEFP.

4. WEFP with a strong lateral effect can be formed by double liners with a suitable material combination. Among several plans, the maximum value of reaming effect can reach 40.4%.

1. B. Liu, H. T. Zhang, and J. T. Li, "Development of the armed helicopter technology," *Ship Electronic Eng.*, **31**, No. 2, 20–23, 34 (2011).

2. G. Kesberg, V. Schirm, and S. Kerk, "Pele – the future ammunition concept," in: Proc. of the 21st Int. Symp. on Ballistics (Adelaide, Australia), Vol. 2 (2004), pp. 1134–1144.

3. G. Paulus, P. Y. Chanteret, and E. Wollmann, "Pele: a new penetrator-concept for the generation of lateral effects," in: Proc. of the 21st Int. Symp. on Ballistics (Adelaide, Australia), Vol. 1 (2004), pp. 104–110.

4. J. B. Men, J. W. Jiang, J. F. Shuai, et al, "Experimental research on formation and terminal effect of explosively formed compound reactive fragments," *Trans. Beijing Inst. Technol.*, **30**, No. 10, 1143–1146 (2010).

5. S. Y. Wang, J. B. Men, and J. W. Jiang, "Research on formation process of wrapping explosively formed compound penetrator," *Chinese J. High Pres. Phys.*, **27**, No. 1, 40–44 (2013).

6. W. Arnold, E. Rottenkolber, and T. Hartmann, "Axially switchable modes warheads," in: Proc. of the 28th Int. Symp. on Ballistics (Atlanta, GA, 2014), Vol. 1 (2014), pp. 289–300.

7. J.-Q. Liu, W.-B. Gu, Y. Tang, and T. Guo, "Numerical investigation on EFP forming performance with variation wall thickness hemispherical liner," *J. PLA Univ. Sci. Technol.*, **9**, No. 2, 172–176 (2008).

8. *Interactive Non-Linear Dynamic Analysis Software: AUTODYN User's Manual*, Century Dynamics Inc., Houston, TX (2003).

9. Y. N. Liu, J. H. Zhu, and H. J. Zhou, "Strength of a low carbon steel at different temperatures strain rates," *Mater. Sci. Progr.*, **4**, No. 4, 285–290 (1990).

10. L. L. Wang and S. S. Hu, "Dynamic stress-strain relations of Al alloy LF6R and AL L4R under high strain rates," *Acta Mech. Solida Sin.*, **2**, 163–166 (1986).